Moisture transport of extreme rainfall events and remote influences of traveling disturbances

Project Representative
Ning Zhao　Center for Coupled Ocean-Atmosphere Research, Research Institute for Global Change, Japan Agency for Marine-Earth Science and Technology

Author
Ning Zhao*1

*1 Center for Coupled Ocean-Atmosphere Research, Research Institute for Global Change, Japan Agency for Marine-Earth Science and Technology

Keywords： Cold surge, Heavy rainfalls, Java Island, Backward trajectories

1. Research Background

As a part of the 'Years of the Maritime Continent', an observation campaign was conducted from 8 Jan to 8 Mar 2021 to investigate the cross-equatorial northerly surges (CENSs) and their influences on the local weather systems [1]. During the two-month campaign, six CENSs were observed and induced a series of heavy rainfalls over Java Island.

As shown in Fig. 1, the northeasterly wind dominated the entire South China Sea (SCS) during the CENSs with a stronger wind core exceeding 8 m/s near the coast of Vietnam. When the surface wind blew into the Maritime Continent, the unique land distributions of the Maritime Continent forced it to turn east before it entered the Java Sea and joined the dominant westerlies south of the Equator. These surges enhanced the cold air advection and surface evaporation, resulting in frequently enhanced southward moisture transport and concentrated rainfalls in the equatorial regions (e.g., Fig. 1b). Nevertheless, compared to the satellite observation, although ERA5 captured the temporal variations of rainfall intensities, it greatly underestimated the severe events. Therefore, this study focuses on three scientific issues: a) factors controlling the heavy rainfalls during the CENSs; b) why ERA5 underestimated them; and c) the role of air-sea interactions in moisture supply to the heavy rainfalls.

2. Experiment Designs and Model Settings

To investigate the heavy rainfalls during the CENSs, we conducted a set of numerical experiments based on uncoupled (WRF) and coupled (WRF-ROMS) models, focusing on the events in mid-February [2]. The integrating period for numerical experiments was set from February 9 to 21, 2021, which covered the heavy rainfalls in mid-February, including the most severe event on February18 (HR18). Our model has a resolution of 9 km and 60 vertical sigma layers from the surface to 50-hPa, with a two-way nested 3-km domain embedded over the Java region. The initial and boundary conditions were obtained from ERA5 and HYCOM. Four sensitivity experiments were conducted, including an uncoupled experiment based on the SST used in ERA5 (NOCP) and two coupled models with higher and lower coupling frequencies (HFCP and LFCP). To evaluate the role of air-sea interaction in moisture supply, we also conducted trajectory analyses based on four experiments following our previous study [3].

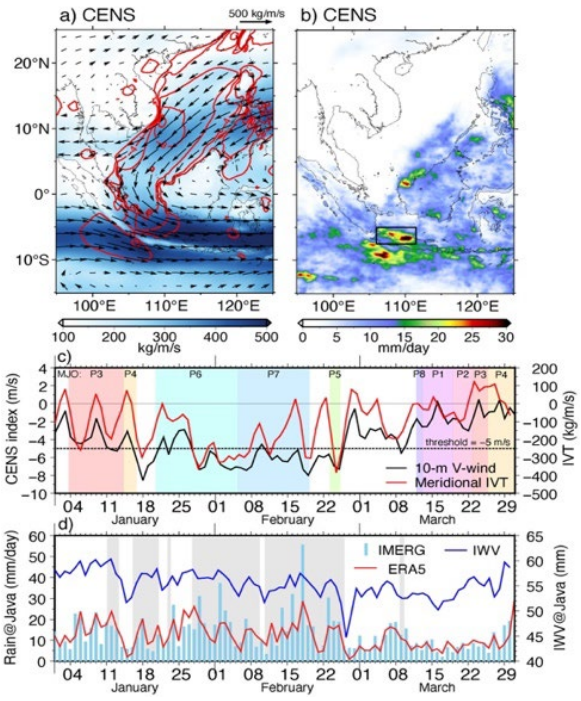

Figure 1: Mean (a) moisture transport (IVT) and (b) satellite-observed rainfalls averaged during the CENSs in Jan-Mar 2021. (c) Time series of meridional wind and meridional moisture transport over 105~110°E, 5°S~0° with (d) moisture content (IWV) and rainfalls over the western Java region.

3. Heavy rainfalls in mid-February

As shown in Fig. 2a, the heavy rainfalls simulated in our models exhibited higher intensities and better temporal variations than those in ERA5, including a much-improved HR18 event. Both the satellite and our models show that, during the CENSs in mid-February, rainfalls over the western Java region exhibited pronounced diurnal variations, which started at about 15 UTC and reached their peaks at 21 UTC, suggesting CENSs enhanced the diurnal cycle of convection over Java Island.

Compared to the clear diurnal variations shown above, although diurnal rainfall in ERA5 presented a similar starting time, it was followed by some short-term variations later and never reached the peak, suggesting the convection was likely initiated in ERA5 but not maintained well. A similar conclusion could be made by comparing the net moisture transport into the region (e.g. Fig. 2b). It was shown that the net moisture inflow, which represents the large-scale moisture convergence, corresponded well with the rainfall intensities, and ERA5 showed the lowest net inflows during all events.

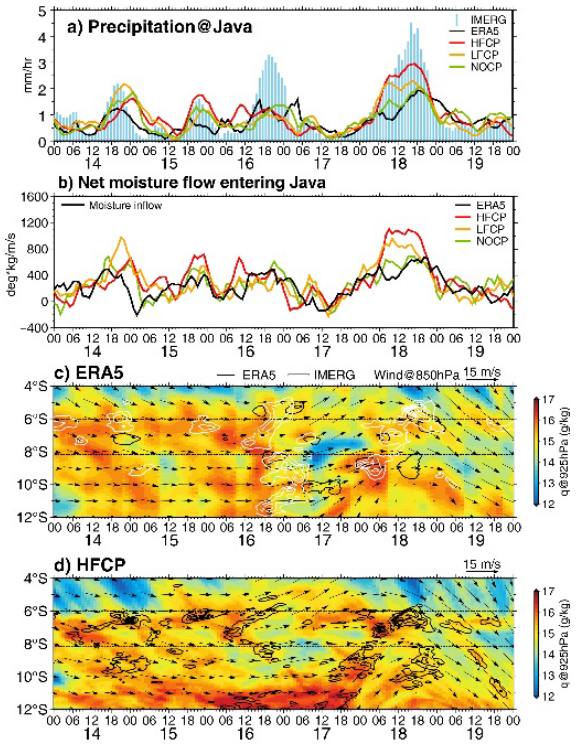

Figure 2: Temporal variations of (a) rainfalls over the western Java region, (b) net moisture inflow, and Hovmöller diagrams of the specific humidity at 925 hPa (q, color) and winds at 850 hPa (vectors) based on (c) ERA5 and (d) HFCP.

Unlike the diurnal-cycle-related events, the HR18 event had a different story, exhibiting a unique bimodal distribution of precipitation and lasting more than 30 hours. It was found that ERA5 did capture the bimodal distribution of precipitation; however, its intensity was only about half of that observed by the satellite. By contrast, our experiments showed comparable or better performance in simulating this event, especially the two coupled ones.

As shown in Fig. 2, this event started at 18 UTC on February 17, and the precipitation continuously increased in the following 12 hours. Interestingly, moisture mainly came from the south during this stage (e.g., Fig. 2c), which was controlled by the northerly inflows in previous events. After that, as the northerly transport became dominant again, the moisture supply from the south was reduced as shown by the nearly disappeared southerly wind after 06 UTC on February. However, that was not the case in the coupled model, where the southerly inflow remained strong and kept playing a positive role for over 12 hours, which maintained the strong moisture inflow. As a result, convection in the two coupled experiments was much enhanced, inducing the second peak at 18 UTC, which was not only underestimated but also a few hours delayed in ERA5 and uncoupled experiments.

Moreover, compared to our simulations, ERA5 showed some unrealistic moisture variations, likely induced by the data assimilation and reanalysis processes. It was shown that, although it was delayed and weak, convection over the mountainous regions was initiated at about 06 UTC in ERA5 (Fig. 2c). However, the appearance of reanalysis-induced dry bias prevented its further development, resulting in the early weakening of precipitation found in ERA5 (Fig. 1a), suggesting the underestimation of ERA5 was also related to such unrealistic dry biases.

4. Moisture source analysis

To provide a quantitative estimation of the role of CENSs in supplying moisture to the HR18 event and how the air-sea interaction modulated such moisture gain/loss processes (i.e., evaporation, precipitation, and water vapor recycling within the troposphere), we conducted a backward trajectory experiment with virtual air parcels released during the event by using the best-performing HFCP (Fig. 3).

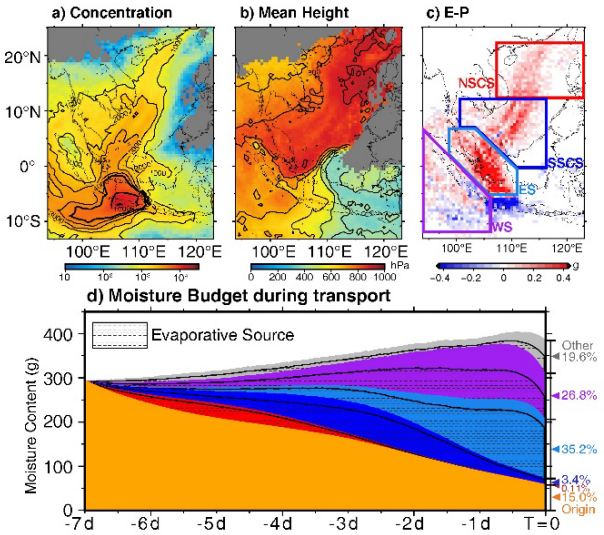

Figure 3: Statistical results based on the trajectories released during the HR18 event in HFCP: (a) particle concentration, (b) mean height, and (c) net surface freshwater flux, along with (d) the budget of their total moisture content with contributions from the four subregions (boxes in panel d): Northern South China Sea (NSCS), Southern SCS (SSCS), east of Sumatra (ES), and west of Sumatra (WS). Properties were estimated using unit columns with a 0.5° mesh size, and only columns with more than 10 particles passed were plotted in panels a-c. In panel d, the moisture sources prior to 7 days and those out of the four subregions are marked as origin and other, respectively, where the evaporative source was defined by the moisture uptake within the planetary boundary layer.

As shown by the two branches in Fig. 3a, our results suggest that the moisture contributed to the HR18 event could be separated into two groups that were coming from the north and southwest, which agreed well with the joint efforts of northerly and

southerly winds we found above. Particularly, the trajectories show that the northern group stayed within the lower levels when they passed the SCS with mean heights below the 800 hPa level, suggesting they were transported by the CENS-related low-level winds. Compared to that, the southwestern group mainly came from the lower-to-mid levels, which was likely due to the active convective activities west of Sumatra.

In addition to their different paths, particles in the two groups also behaved differently in their moisture gain processes. In the northern group, most of the moisture was supplied by the surface evaporation from the SCS, the offshore regions of Sumatra, and the western Java Sea, as shown by their large proportions of evaporative source (Fig. 3d). Among these regions, moisture from the eastern coastal region of Sumatra contributed the most (~35%), and 85% of that was obtained by surface evaporation (Fig. 3b). Similarly, the evaporative source also dominated the moisture contribution from the SCS (~3.5%), but most of that was lost during the southward transport, especially for those from the northern SCS. By contrast, only half of the moisture was supplied by surface evaporation in the southwestern group, while the other half was gained by the water vapor recycling related to the convective activities there (e.g., Fig. 1). Note that although about one-third of the moisture could not be identified due to the time limitation of backward tracing and the coverage of our model domain and subregions (Origin and Other in Fig. 3b), our results still demonstrated the important role of CENSs in supplying moisture (~40%, i.e., the sum of SCS and ES regions).

By comparing the four experiments, the uncoupled experiments showed relatively larger final contributions of SCS, even though their peaks were lower. Meanwhile, contributions of surface evaporation in uncoupled experiments were only about 60% of that in coupled ones. Therefore, the air-sea interaction enhanced the surface evaporation and the convective activities, leading to more active gain/loss processes of moisture and, consequently higher contributions of regions nearby.

References

[1] Moteki, Q. Vertical structure and occurrence patterns of the cross-equatorial northerly surge under different ENSO and MJO phases. *Sci. Rep.*, 14, 29116. (November 2024)

[2] Zhao, N., & Nasuno, T. How does the air-sea coupling frequency affect convection during the MJO passage? *J. Adv. Model. Earth Syst.*, 12, e2020MS002058. (March 2020)

[3] Zhao, N., et al. Moisture sources of the Tohoku heavy rainfalls in August 2022 and the influences of tropical storms. *Geophys. Res. Lett.*, 50, e2023GL104166. (September 2023)